scientific reports

Check for updates

OPEN

Antioxidant effects of silver-ceria nanoparticles on the reduction of melanin in amelanotic melanoma cell biology

Masoumeh Ghorbani[1], Nafise Sepahdoost[2], Zahra Vaezi[3]✉, Danial Kahrizi[4]✉ & Hossein Naderi-Manesh[2]✉

Although cerium oxide nanoparticles (nanoceria, CeO_2) have a wide range of applications, it is imperative to consider their significant implications for human health. In particular, modifying the surface properties of CeO_2 is of great importance in biomedical applications. In this study, a conventional wetness incipient impregnation technique was employed to load silver (Ag) metal onto the surface of CeO_2 NPs synthesized via the hydrothermal method. Then, the antioxidant effects of silver-cerium oxide nanoparticles (Ag@CeO_2 NPs) were evaluated on the melanin content of A375 skin cancer cells. The synthesized nanoparticles have been identifed using combined characterizations of the hydrodynamic size, zeta potential FTIR, FE-SEM, and UV-Vis spectra. The average particle size of Ag@CeO_2 NPs was measured at 234 ± 20 nm with the zeta potential value − 33.5 mV. FE-SEM image revealed that Ag@CeO_2 nanoparticles were polyhedral particles consisting of cubic nanostructures with rounded corners. The antioxidant capability of Ag@CeO_2 NPs was assessed using DPPH and ABTS assays and the inhibitory effects of that on melanin biosynthesis (extracellular and cellular melanin content) were examined on human melanoma cell line. Overall, the results provide promising baseline information for the potential applications of Ag@CeO_2 NPs in treating hyperpigmentation in the skin.

Keywords Antioxidant activity, Ag@CeO_2 nanoparticles, A375 melanoma cells, Melanin regulation, Hydrothermal synthesis

The imbalanced electrons associated with oxygen can engage in reactions that yield partially reduced, highly reactive species, collectively referred to as reactive oxygen species (ROS). Examples of ROS include hydroxyl radicals (.OH), superoxide anions ($.O^{-2}$), and hydrogen peroxide (H_2O_2)[1]. These species are typical byproducts of aerobic metabolism, arising from processes such as the mitochondrial electron transport chain, cytochrome P450 activity, the NADPH oxidase complex, and peroxisomal functions. Due to their elevated chemical reactivity, ROS are transient species that can induce lipid peroxidation, enzyme oxidation, protein modification, and DNA mutations. Aerobic organisms have developed various chemical and enzymatic antioxidant mechanisms to mitigate the potential damage caused by oxidative stress. Key antioxidant enzymes include superoxide dismutase (SOD), glutathione peroxidase (GPx), and catalase (CAT). SOD facilitates the dismutation of superoxide radical anions into hydrogen peroxide and oxygen, while CAT and GPx are responsible for the conversion of hydrogen peroxide into water[2]. Cerium oxide nanoparticles (nanoceria, CeO_2), which represent the oxidized form of the rare element cerium, have been shown to mimic the activity of SOD due to alterations in surface oxygen vacancies and valence configurations. Consequently, these nanoparticles can function as scavengers of ROS across various biological contexts[3]. The nanoscale properties of cerium oxide are enhanced due to the increased surface-to-volume ratio characteristic of nanoparticles, which has led to numerous prospective applications in biomedicine. These applications encompass endothelial cell protection, wound healing, anticancer strategies, and optical biosensors for the inflammation-related diseases[4–6]. Research into the biological applications of nanoceria is expanding rapidly. Antioxidants present a potentially promising avenue for the prevention and treatment of melanoma, as the further induction of oxidative stress may facilitate the gradual demise of malignant cells. As

[1]Department of Nanobiotechnology, Faculty of Strategic Sciences and Technologies, Razi University, Kermanshah, Iran. [2]Department of Nanobiotechnology, Faculty of Biological Science, Tarbiat Modares University, Tehran 14115-154, Iran. [3]Department of Bioactive Compounds, Faculty of Interdisciplinary Sciences and Technologies, Tarbiat Modares University, Tehran 14115-154, Iran. [4]Department of Biotechnology, Faculty of Agriculture, Tarbiat Modares University, Tehran, Iran. ✉email: zahra.vaezi@modares.ac.ir; dkahrizi@modares.ac.ir; naderman@modares.ac.ir

a result, both antioxidants and prooxidants may play a role in interventions for melanoma. On the other hand, Silver Nanoparticles (Ag NPs) stabilized with antioxidants like epigallocatechin gallate (EGCG), demonstrated cytotoxic effects on melanoma cells by inducing oxidative stress and damaging cellular components, leading to apoptosis[7].

It is important to note that the mechanisms and effects of melanin on oxidative stress within the context of melanogenesis remain incompletely understood. The incorporation of zinc and copper complexes into both unloaded and vitamin E-loaded nanoparticles has been shown to enhance antioxidant properties while effectively inhibiting melanin production. This approach holds potential for the treatment of disorders associated with melanogenesis. But such these studies have not specifically focused on their ability to reduce melanin content in melanoma cells[8,9]. While the production of melanin can induce oxidative stress, melanin possesses unpaired electrons, allowing it to function as an antioxidant by interacting with free radicals and other reactive species, thereby mitigating their effects[10]. Melanin exhibits a hydrophobic complex structure with a negative charge, resulting from the oxidation and polymerization of phenolic compounds, and is synthesized in melanocytes and melanosome cells[11]. The production and distribution of melanin can be diminished by inhibiting the enzyme tyrosinase; however, complete cessation of melanin production is not feasible, as it is a physiological process, and halting this process may result in depigmented skin areas. Tyrosinase serves as a critical enzyme in melanin biosynthesis, and numerous effective molecules, including phenolic extracts, flavonoids, terpenoids, and alkaloids, have been identified as inhibitors of this enzyme or as agents for skin-lightening[12]. Several factors can contribute to an increase in skin melanin levels. Melanin can accumulate in the skin, leading to darkening and the formation of dark spots. These spots may arise from various causes, including sun exposure, hormonal changes, skin aging, and liver issues. Freckles are a specific example of localized melanin accumulation that results in dark spots[12]. The development of novel nano-sized molecules with significant potential to reduce melanin levels for use in skincare products aimed at treating skin disorders such as hyperpigmentation is a primary objective of ongoing research in this domain. This study specifically examines the antioxidant effects of silver – cerium oxide nanoparticles ($Ag@CeO_2$ NPs) in reducing melanin levels in A375 melanoma cancer cells (scheme 1).

Materials and methodology

Chemicals and Reagents

The $Ce(NO_3)_3.6H_2O$ (99.5%) and $AgNO_3$ (> 99.8%) salts bought from Sigma-Aldrich, and ammonia (NH_4OH, 25%) have been applied for the synthesis of $Ce_{1-x}Ag_xO_2$ nanoparticles as cerium and silver precursors, and stabilizing agent, respectively. All other chemicals were acquired from commercial sources and utilized in their original form without any further purification processes. Furthermore, the A375 human melanoma cell line was sourced from the National Cell Bank of Iran (Pasteur Institute).

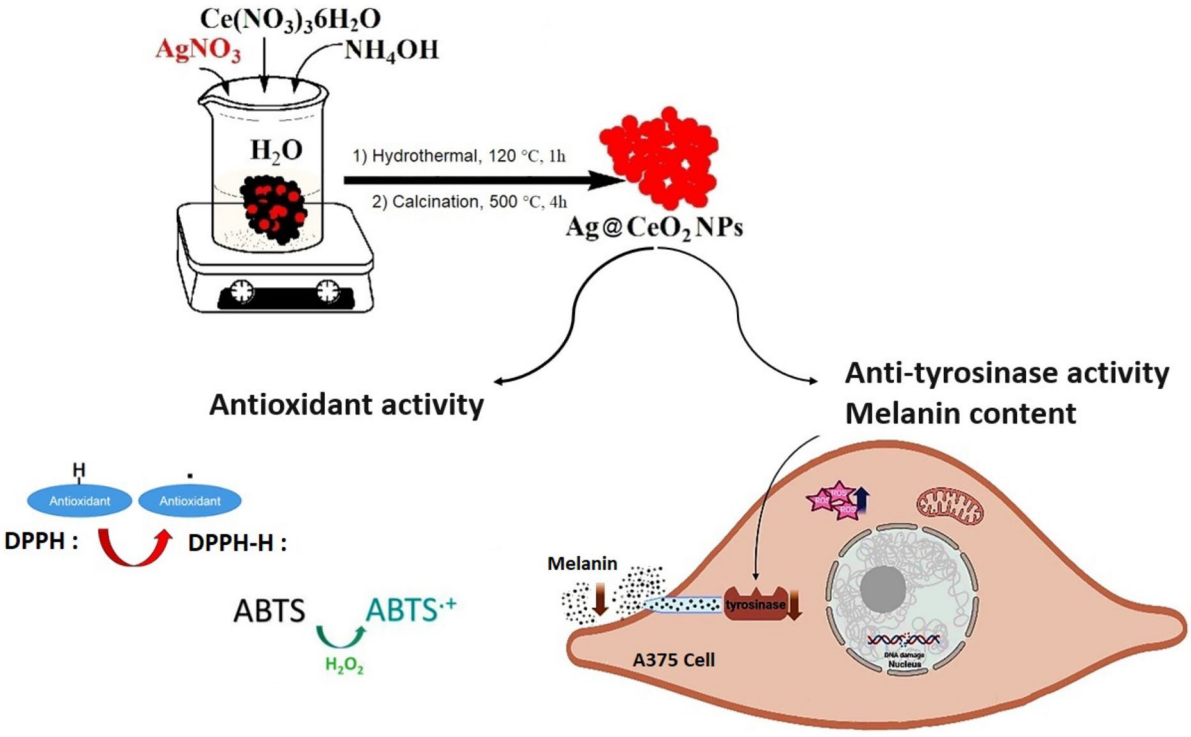

Scheme 1. Silver-cerium oxide nanoparticles: Synthesis method and application in the melanin content reduction.

Synthesis of Ag@CeO_2 NPs and Characterization

The synthesis of Ag@CeO_2nanoparticles (NPs) was conducted according to the procedure described in the literature[13]. Initially, a solution of 3.53 g of ammonia (NH_4OH, 25%) was introduced to a pre-prepared mixture consisting of 4.85 g (11.169 mmol) of cerium nitrate hexahydrate ($Ce(NO_3)_3.6H_2O$) and 2.963 g (17.44 mmol) of silver nitrate ($AgNO_3$) dissolved in 20 mL of water, which was subsequently diluted with an additional 12 mL of water. The resultant mixture was vigorously stirred at 300 revolutions per minute (rpm) for 2 min at room temperature. Following this, the resulting black coprecipitate underwent heat treatment in an autoclave under steam conditions at 120 °C for 10 min. The resulting golden-brown solid was separated via centrifugation and then subjected to calcination at 500 °C for 4 h in an air atmosphere.

The synthesized Ag@CeO_2 NPs underwent extensive evaluation using a variety of analytical techniques. Absorption spectra were obtained using ultraviolet–visible or/and (UV-Vis) spectroscopy. The average hydrodynamic size with polydispersity index (PDI), and zeta potential of Ag@CeO_2 nanoparticles in media was determined by dynamic light scattering (DLS) (Nano-ZetaSizer-HT, Malvern Instrument). The functional groups of the synthesized nanoparticles were determined using Fourier transform infrared (FTIR) spectroscopy (Bruker Tensor 27 Spectrometer Bruker, Japan) from 4000 –400 cm^{-1}, and using dried samples and KBr pellets. The morphological characterization of Ag@CeO_2 nanoparticles (NPs) was conducted using a field-emission scanning electron microscope (SEM, Quanta 450, FEI, USA).

Antioxidant potential evaluation of Ag@CeO_2 NPs

DPPH assay

Antioxidant Activity was acceseed via DPPH (2,2-diphenyl-1-picrylhydrazyl) Assay. To assess the antioxidant capacity in terms of DPPH radical scavenging, a solution of 1 mg of DPPH was initially prepared by dissolving it in 17 ml of ethanol, resulting in a purple DPPH solution[14]. Various concentrations of Ag@CeO_2 NPs (0.05, 0.1, 0.5, 1, and 3 mg/ml) were examined for their antioxidant efficacy. The reaction mixture comprised 400 µl of the DPPH solution and 100 µl of the respective concentrations of Ag@CeO_2 NPs. The mixture was subjected to vigorous shaking and subsequently incubated at room temperature for 40 min, after which the absorbance was recorded at 517 nm. The control sample included all compounds except the Ag@CeO_2 NPs, with ascorbic acid as the standard reference. The final percentage of inhibition was determined using Eq. (1):

$$\text{Inhibition } (\%) = \frac{\text{Absorbance of control } - \text{ Absorbance of sample}}{\text{Absorbance of control}} \times 100 \quad (1)$$

ABTS assay

In the ABTS (2,2'-Azinobis (3-ethylbenzothiazoline-6-sulfonic acid) diammonium salt) assay, initial stock solutions of 2.4 mM potassium persulfate and 7mM ABTS were prepared. The working solution was created by combining equal volumes of the two stock solutions and allowing them to react for 15 h at room temperature in a dark place[15]. The solution was then diluted by mixing the $ABTS^+$ solution with water to achieve an absorbance of 1.00 ± 0.02 units at 734 nm, as measured by a spectrophotometer. A fresh $ABTS^+$ solution was prepared for each assay. Various concentrations of a standard ascorbic acid solution were also prepared. Subsequently, 100 µl of Ag@CeO_2 NPs at different concentrations (0.05, 0.1, 0.5, 1, and 3 mg/ml) were allowed to react with 400 µl of the $ABTS^+$ solution for 3 h in a dark setting. The absorbance was then measured at 734 nm. All measurements were performed in triplicate, and the results were averaged. The means were compared using Duncan's multiple range test ($P < 0.05$). The final percentage of inhibition was calculated using Eq. (1).

Cell culture of amelanotic melanoma lines

The A375 melanoma cell line was cultured in Dulbecco's Modified Eagle's Medium (DMEM, Gibco, MA, USA), which was supplemented with 10% fetal bovine serum and 1% penicillin/streptomycin (Wisent, Montreal, Canada). The cells were maintained in a humidified incubator with an atmosphere of 5% CO_2 at a temperature of 37 °C.

MTT assay

The MTT assay was conducted to evaluate the viability of the A375 cell line exposed to the synthesized materials. This colorimetric assay relies on the ability of mitochondrial enzymes in viable cells to reduce the tetrazolium salt (MTT) to insoluble purple formazan crystals. The intensity of the color correlates with the number of viable cells. A375 cells were cultured in DMEM high glucose medium supplemented with 10% FBS and 1% penicillin/streptomycin. Subsequently, 5000 cells per well were seeded into a 96-well plate and allowed to adhere overnight. The following day, the wells were observed to confirm uniform seeding and cell attachment. The cells were then treated with the prepared concentrations for 24, 48, and 72 h. After the treatment periods, the media were removed, and the MTT solution (0.5% w/v in FBS-free medium) was added to the cells. The plates were incubated at 37 °C with 5% $CO_2$for 3 h to allow the mitochondrial reduction of MTT. The resulting formazan crystals were dissolved with 100 µl of DMSO, and the absorbance was measured at 570 nm using an ELISA plate reader[16]. This assay was performed in quadruplicate to ensure accuracy.

Melanin content measurement

The both intracellular and extracellular melanin content in A375 cell lines were evaluted using absorbance measurements. For this purpose, 10^4cells were seeded into a 48-well plate and allowed to adhere to the surface. To ensure that phenol red in the medium did not interfere with tyrosine, the amino acid precursor of melanin, RPMI medium without phenol red was used. Subsequently, 0, 50, and 100 µg/mL of the nanomaterial were

added to the medium after removing the existing medium from each well. The extracellular melanin was then measured at 490 nm using an ELISA plate reader to generate the melanin curve[17]. To measure intracellular melanin content, cells were incubated with 1 N NaOH containing 10% DMSO for 1 h at 80 °C, and then intracellular melanin production was measured at different time points at 405 nm.

Statistical analysis

All experiments were conducted in triplicate, and the findings were subsequently reported. The experimental data were subjected to analysis utilizing SPSS software. A statistical significance threshold was established at $p < 0.05$.

Results and discussion

Characterization of silver – cerium oxide nanoparticles (Ag@CeO_2 NPs)

The synthesized Ag@CeO_2NPs were subjected to an extensive evaluation employing various analytical techniques and the ability to absorb light can be effective in estimating photocatalytic and antioxidant effects. In some characterization spectra, CeO_2 nanoparticles are used for comparison. They characterized in terms of mean size, ζ-potential, polydispersity index (PDI), and morphology. As shown in Fig. 1a, the UV-Vis absorption spectra of pure CeO_2 and the heterostructured Ag@CeO_2NPs in a wavelength region ranging from 200 to 800 nm. The photo-absorption of pure $CeO_2$is located in the UV region with two dominant absorption peaks, the maximum appeared at about 300–330 nm and other at 230 nm, which was related to the charge transfer from O (2P) to Ce (4f) orbitals[18,19]. While, the spectral patterns of Ag@CeO_2NPs heterostructured photocatalysts show the steep absorption edge in the UV region and much strong absorption shifted to the visible light region. This phenomenon can be attributed to the surface plasmon resonance (SPR) effect of Ag metal. The Visible-Region Band (380–400 nm): Attributed to the surface plasmon resonance (SPR) of metallic Ag nanoparticles, a phenomenon widely reported in Ag-doped metal oxides[20,21]. The plasmonic Ag metal, has extended the light absorption toward visible light region, conforming the successful loading of Ag on the surface of CeO_2photocatalysts. These results are in line with a study that found the ability of visible light absorption regularly increases with increasing Ag content[22]. The SPR effect enhances visible-light absorption by Ag@CeO_2NPs, which directly impacts their antioxidant activity. This aligns with recent studies showing that plasmonic nanoparticles amplify redox-modulating capabilities through localized electric fields[23].

The hydrodynamic mean diameter of the Ag@CeO_2 NPs was 234 ± 20 nm, with a (PDI = 0.276), indicating a colloidal suspension with a relatively uniform size distribution. Additionally, the zeta potential of the Ag@CeO_2 NPs (−33.5 mV) was measured at pH = 7.4, suggesting favorable stability for the nanoparticles Fig. 1b. The higher zeta potential of the Ag@CeO_2 NPs suggests that the NPs possessed an enhanced resistance to aggregation and thus improved morphological stability and mechanism for cellular interactions.

As shown in Fig. 2, the chemical texture and the surface functional groups of pure CeO_2 and the heterostructured Ag@CeO_2 are detected using FTIR spectra at the wave number range of 400–4000 cm^{-1}. The spectral pattern of pure CeO_2 demonstrates a strong absorption band at 482 cm^{-1} corresponding to metal–oxygen bonds and the weak absorption band emerged at 880 $cm^{-1}$is also attributed to the Ce–O stretching

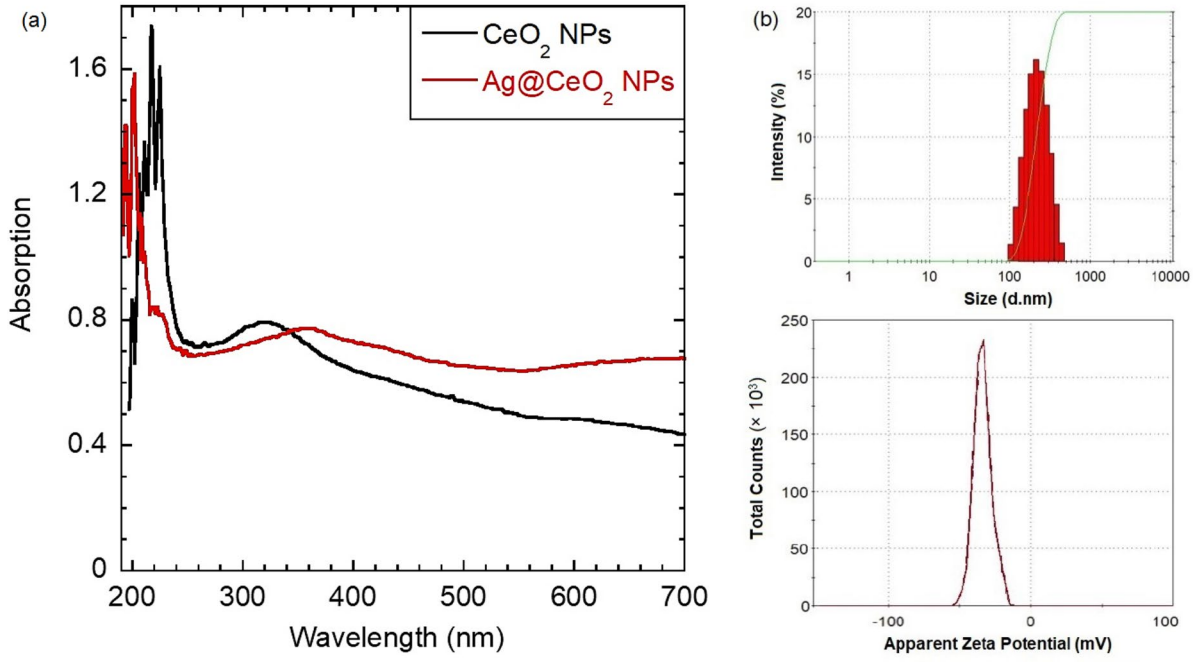

Fig. 1. (**a**) UV–Vis absorption spectra of pure CeO2 and Ag@CeO2 heterostructured photocatalysts (**b**) Particle size distribution and zeta potential value for Ag@CeO_2 NPs.

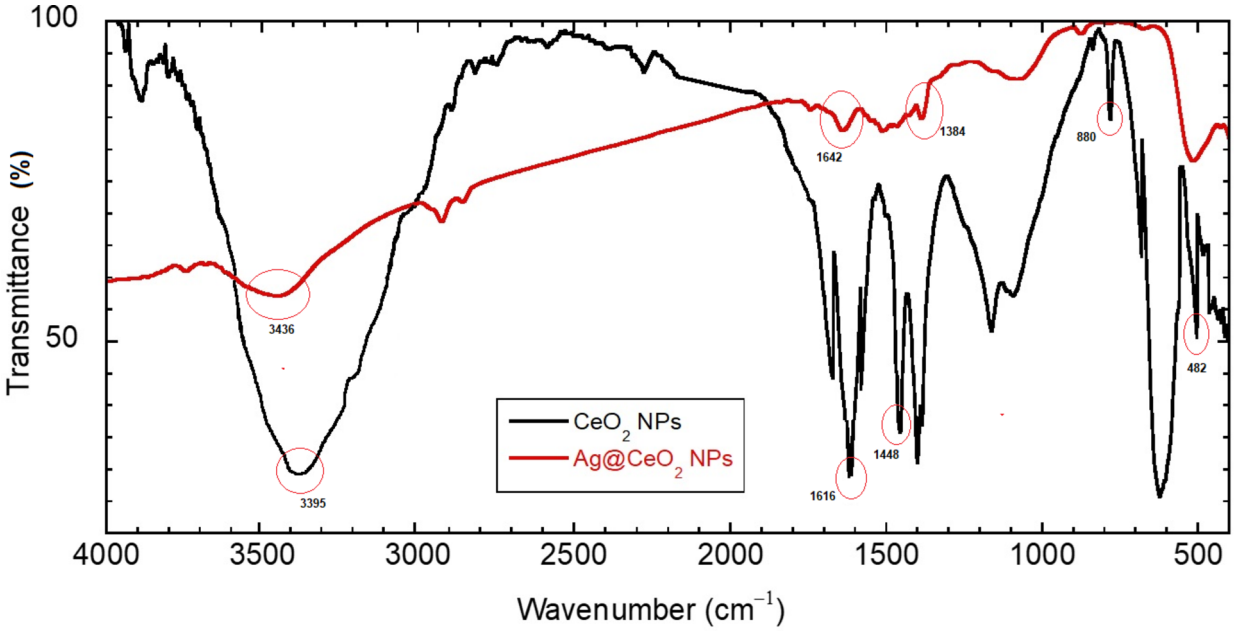

Fig. 2. FT – IR Spectra of pure CeO_2 and the heterostructured Ag@CeO_2 NPs.

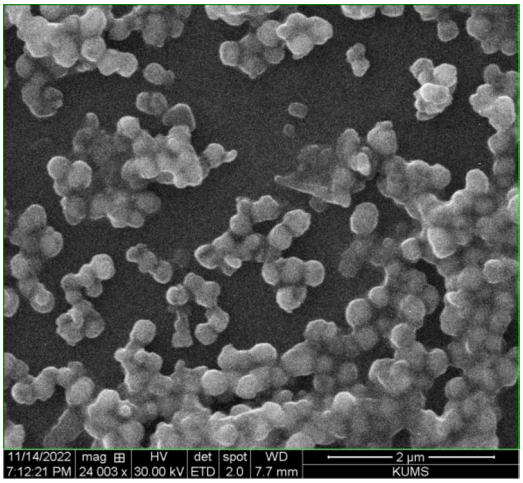

Fig. 3. SEM image of Ag@CeO_2 NPs.

vibration[24]. The both of them are shifted to 514 cm^{-1} and 1083 cm^{-1}, respectively, in the spectrum of Ag@CeO_2 NPs.

The spectral patterns of Ag@CeO_2 indicate two new absorption bands at 1384 and 1616 cm^{-1} are related to the presence of the nitrate group and the bending vibration of adsorbed water, respectively, appearing instead of the band disappeared at 1448 cm^{-1}, originated from CO_2 adsorbed on the CeO_2 surface, as compared to that of pure CeO_2 [22,25]. Additionally, the absorption bands at1642 cm^{-1} correspond to physically adsorbed water molecules and there is a shift in the absorption band relevant to OH stretching vibration of hydroxyl groups at 3395 cm^{-1} that moves to higher wave numbers at 3436 cm^{-1}. This shift can be explained based on dative covalent bonds formed between Ag and Ce with O. The covalent bond made between Ag and O is stronger compared to that formed between Ce and O. The stronger Ag–O bond leads to an enhancement in the bond strength of hydroxyl groups formed on the surface of Ag@CeO_2 and as a result leads to a shift toward higher wave numbers. The changes observed at Ag@CeO_2 spectrum well verify the successful Ag loading on the surface of CeO_2.

Figure 3 illustrates FE-SEM image relevant to the heterostructured Ag@CeO_2 NPs and the particle sizes are estimated by (ImageJ). It seems that NPs exhibit a spherical morphology and aslo a relatively uniform cubical-like nanostructure with rounded corner with an average size of about 157 nm.

It is obvious that the Ag loading on the surface of CeO_2 shows no recognizable change on the surface morphologies as compared to that of pure CeO_2, which reported previously[25]. However, the loaded silver effected an enhancement in particle sizes, which are in good agreement with literature[22].

Antioxidant activity for free radical scavenging.

The antioxidant potentials of $Ag@CeO_2$ NPs were measured by different chemical assays: DPPH assay and ABTS assay. Both assays have been widely used to determine the free radicalscavenging activity of various pure compounds and plants. The scavenging effect on DPPH radicals assay showed concentration-dependent activity (Fig. 4a), For example, the maximum antioxidant activity of ceria-silver nanoparticles at a concentration of 0.1 mg/ml was measured at 81%, however, for ascorbic acid (standard sample) was only 38% at this concentration. The results showed that ceria-silver nanoparticles possess a strong ability to scavenge DPPH free radicals. Furthermore, the experiment revealed that ceria silver nanoparticles exhibited higher antioxidant activity at lower concentrations, demonstrating an inverse relationship between concentration and antioxidant effect.

The research conducted by Ravichandran et al. showed that silver nanoparticles exhibit DPPH radical inhibition activity, achieving a maximum antioxidant effect of 91.83% at a concentration of 50 µg/ml[26]. Another study by Soren et al. showed that synthesized CeO_2nanoparticles displayed DPPH radical scavenging activity within a concentration range of 25 to 75 ng/ml. However, their activity was significantly diminished at a concentration of 100 ng/ml, falling below the level observed at 25 ng/ml[27]. Our results align with previous research indicating that antioxidant activity decreases at high concentrations of ceria silver nanoparticles.

The ABTS assay is based on the generation of a blue/green $ABTS^+$ that can be reduced by antioxidants. The $ABTS^+$ assay evaluates the ability of antioxidants to scavenge reactive oxygen species (ROS) produced by $ABTS^+$. The $ABTS^+$ radicals are produced through a vigorous reaction between the $ABTS^+$salt and the potent oxidizing agent potassium persulfate. A reduction in absorbance signifies an enhancement in the antioxidant scavenging ability[28]. The green $ABTS^+$ solution changes to a pale yellow and eventually becomes colorless. The radical cation scavenging activities of $Ag@CeO_2$ NPs on ABTS radicals demonstrates that the highest percentage of inhibition of $ABTS^+$ radicals, achieved with ceria silver nanoparticles at a concentration of 0.05 mg/ml, is 48% (Fig. 4b). Conversely, the lowest antioxidant effect, characterized by a 16% inhibition of free radicals, was observed at 0.5 mg/ml. The results of this assay, akin to the DPPH method, indicate that ceria silver nanoparticles exhibit superior antioxidant activity at lower concentrations. Therefore, the enhanced antioxidant activity can be due to the plasmonic excitation facilitates electron transfer from Ag to CeO_2, stabilizing Ce^{3+}/Ce^{4+} redox cycling. This synergistically boosts ROS scavenging, as evidenced by our DPPH/ABTS results (84% inhibition at 3 mg/mL). The similar results are observed by presence of Ag nanoparticles that enhances the light absorption of TiO_2, facilitating the generation of ROS that contribute to antioxidant activity[29]. The interaction between Ag and TiO_2promotes efficient electron transfer, which is crucial for the reduction of free radicals, thereby improving antioxidant effects[30].

Cell viability of $Ag@CeO_2$ Nanoparticles in A375 Cells

The MTT assay is a colorimetric method employed to assess cellular metabolic activity, indicating cell viability and proliferation. The results demonstrated a dose and time-dependent cytotoxicity after exposure to $Ag@CeO_2$ nanoparticles in A375 cells. As shown in Fig. 5, the viability of A375 cells treated with different concentrations of ceria silver nanoparticles (0.5, 1, 5, 10, 50, 100, and 1000 µg/ml) compared to the control group.

Notably, after 72 h, no toxicity was observed across the different concentrations. Additionally, the results at 24 and 48 h were consistent with those at 72 h, indicating that these concentrations did not cause significant cell death. The findings suggest that a 1000 µg/ml concentration of ceria silver nanoparticles is safe and non-toxic for A375 skin cancer (melanoma) cells. Young et al. demonstrated that cerium oxide nanoparticles were not

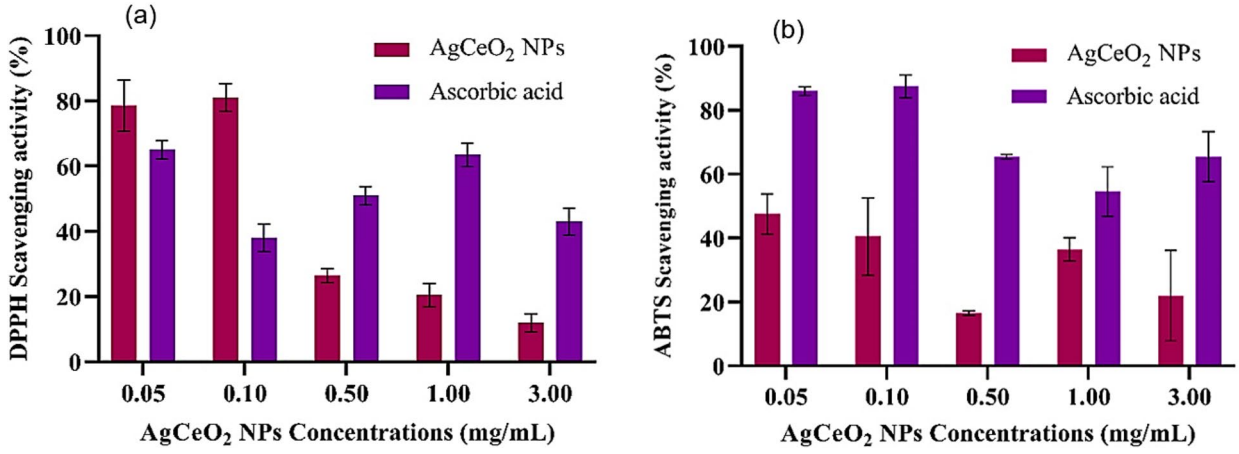

Fig. 4. Evaluation of the antioxidant activity and scavenging effect of ceria silver nanoparticles on (**a**) DPPH and (**b**) ABTS. Each value (%) is expressed as mean ($n = 3$) ± standard deviation.

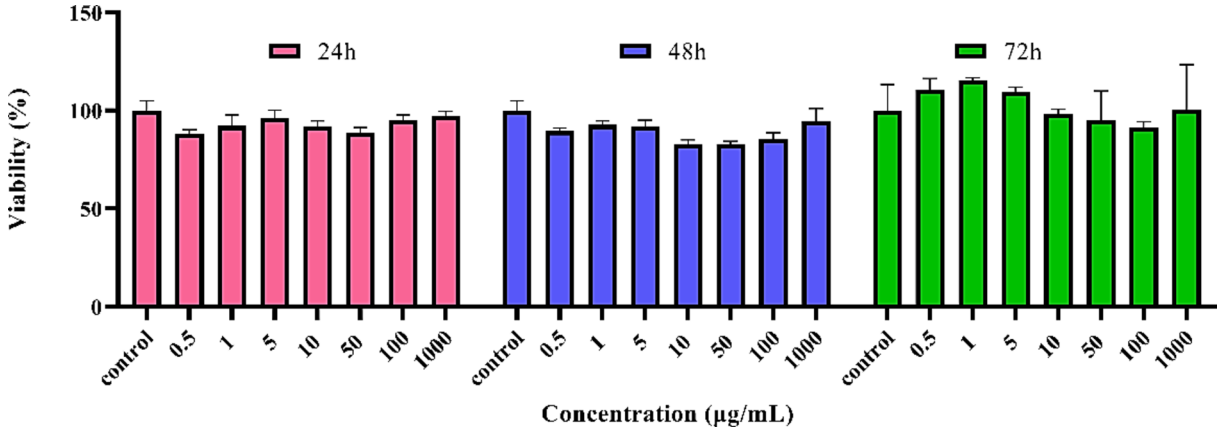

Fig. 5. Percentage cell viability at different concentrations of **ceria silver nanoparticles** in A375 cells for 24, 48 and 72 h, as assessed by MTT assay. Each value represents the mean ± SE of three experiments.

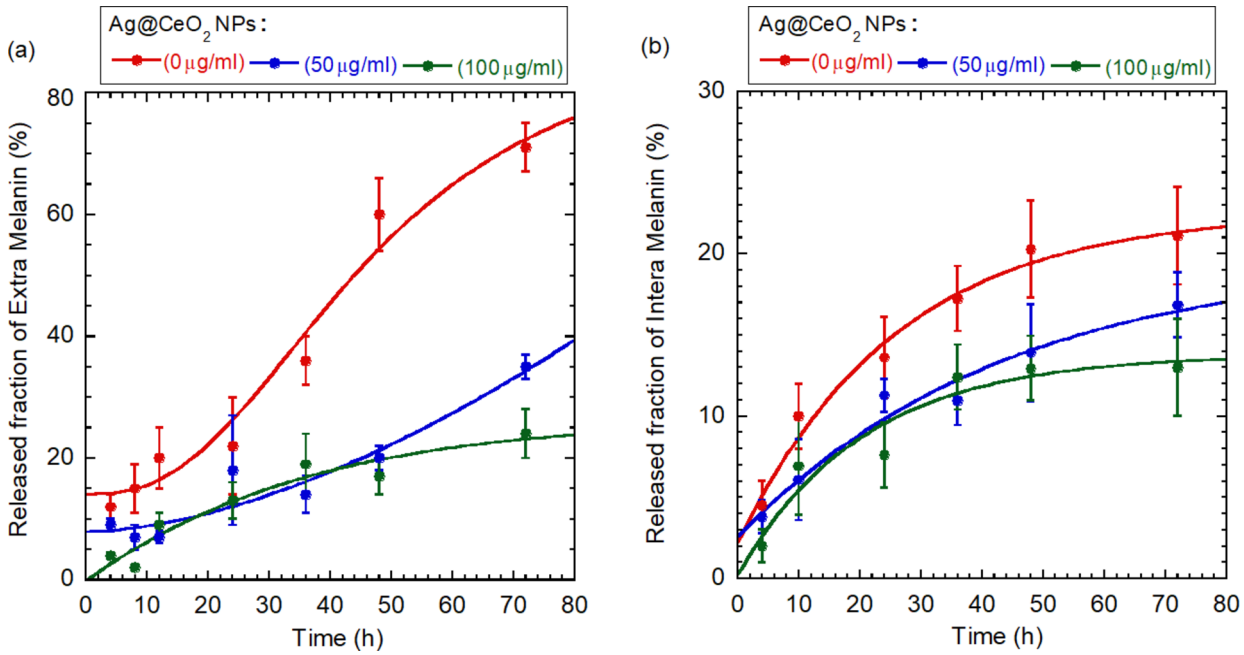

Fig. 6. The effect of ceria-silver nanoparticles on the release of (**a**) extracellular and (**b**) cellular melanin content in A375 cells.

cytotoxic to a human melanoma cell line (Mel1007) at doses up to 400 µg/ml. Furthermore, these nanoparticles were found to reduce intracellular ROS levels[31].

Intracellular and extracellular melanin content assay

Melanin is derived from the amino acid tyrosine, however it is not made from amino acids and is not a protein. It is a pigment produced in a specialized group of cells known as melanocytes. Based on the results obtained from the cytotoxicity assay and the antioxidant activity of ceria silver nanoparticles, the concentrations of 50 and 100 µg/ml were selected to measure changes in melanin production. It is note that, due to the presence of the tyrosine, which is a precursor of melanin, this stage of culture was performed with RPMI culture medium without phenol red dye, which does not interfere with melanin absorption. Initially, by visual observation of the color of the supernatant melanin content, it was determined that melanin production in the culture medium was significantly reduced when cells were treated with the selected concentrations of Ag@CeO_2 NPs.

As illustreated in Fig. 6a, the accumulated extracellular melanin, which corresponds to its release into the culture medium over time (4, 8, 12, 24, 36, 48, and 72 h), measured by absorbance at 490 nm.

As anticipated, during the measurement period, the amount of extracellular melanin produced by A375 cells in the absence of ceria-silver nanoparticles exhibited an upward trend. In contrast, this increase was inhibited in the presence of the two concentrations of ceria silver nanoparticles (50 and 100 µg/ml), resulting in a significant

decrease. Specifically, the change in melanin secretion over time (release kinetics over 72 h) in the presence of nanoparticles at a concentration of 100 µg/ml reached a plateau of 20%, with a very low slope. This finding indicates the effectiveness of this concentration in reducing melanin derived from amino acids, tyrosine, which suggests the antioxidant effect of these nanoparticles. On the other hand, the SPR-induced ROS scavenging disrupts tyrosinase activity and melanosome maturation. This aligns with Yi et al., who identified oxidative stress modulation as a key strategy for melanoma management[32].

Regarding the diverse roles of melanin in the fitness and survival of insects, a study conducted by Phatak et al. examined the effects of silver oxide nanoparticles on melanin levels in Drosophila. The results indicated that silver oxide nanoparticles exert a melanin-modulating effect[33]. Additionally, other study demonstrated that silver nanoparticles function as a whitening agent by decreasing the melanin content in the SK-MEL cell line and serve as significant inhibitors of tyrosinase activity[34]. Also, the melanin content inside the cell (Fig. 6b), which after cell lysis in alkaline medium, the intracellular melanin release was measured at 405 nm[35]. After the first day of incubation Ag@CeO_2 NPs, the amount of melanin increased by over about 10% and reached to 15% during the following day in comparison with control; thus, the intensity of melanization decreased by half within 3 days .

The use of nanoparticles in melanoma treatment not only targets cancer cells effectively but also minimize damage to surrounding healthy tissues, showcasing their potential as a safer alternative to conventional therapies[36]. While conventional antioxidants and depigmenting agents have demonstrated efficacy in treating hyperpigmentation, Ag@CeO_2 NPs offer several potential advantages related to enhanced efficacy, targeted delivery, and sustained release, which we elaborate on below:

Enhanced ROS Scavenging; as demonstrated in our study, Ag@CeO_2 NPs exhibit potent antioxidant activity, with 84% DPPH radical scavenging at 3 mg/mL. The combination of Ag and CeO_2 creates a synergistic effect, where Ag enhances the redox cycling of CeO_2 (Ce^{3+}/Ce^{4+}), leading to more efficient ROS scavenging. Conventional antioxidants like ascorbic acid or glutathione may not offer the same level of synergistic activity. Also, the plasmon resonance of Ag facilitates the ROS scavenging by visible-light absorption. This is a property not present in conventional antioxidants. Ag loading on the surface of CeO_2 nanostructures has decreased minimum optical energy required for generating light-induced electron–hole pairs in the heterostructured Ag@CeO_2 photocatalysts in comparison with that of pure CeO_2 sample, contributing of two mechanisms of charge transportation.

The first mechanism can be ascribed to the surface plasmon resonance (SPR) phenomenon of metallic Ag[37]. The second mechanism can be explained based on the interfacial electron transfer process, such as excitonic charge separation created by the Schottky junction efectively decreases the recombination rate of photoexcited electron–hole pairs and extends the life span of the charge carriers[38]. The previous studies have also shown that cerium oxide nanoparticles can reduce intracellular ROS and hydrogen peroxide levels in cells. ROS can influence melanin synthesis by regulating tyrosinase activity. Furthermore, these nanoparticles possess antioxidant properties that may impact melanin synthesis[39].

Ag@CeO_2NPs showed remarkable antioxidant capacity according to DPPH and ABTS and reducing power assays, suggested the potential use in the treatment of diseases associated with oxidative stress, such as cardiovascular diseases, atherosclerosis, arthritis, Parkinson, and cancer[40,41]. The mechanism of melanin degradation in the presence of Ag@CeO_2 NPs is described by the formation of the hydroxyl radical (OH), which is through either electrons captured by atmospheric oxygen (O_2) or holes trapped by the surface hydroxyl groups (OH^-) and adsorbed water molecules (H_2O). The hydroxyl radicals are extremely strong oxidants, which efectively degrade organic chemicals under visible light irradiation. Hence, the plausible mechanistic pathway of photodegradation performances of the heterostructured Ag@CeO_2photocatalysts can be proposed as the following reactions[22].

$$[\mathrm{Ag@CeO2}] + \mathrm{hv} \rightarrow [\mathrm{Ag@CeO_2}(\mathrm{e}^- + \mathrm{h}^+)]$$

$$[\mathrm{Ag@CeO2}(\mathrm{e}^-)] + \mathrm{O_2} \rightarrow [\mathrm{Ag@CeO_2}] + \mathrm{O_2^-}$$

$$[\mathrm{Ag@CeO_2}(\mathrm{h}^+)] + \mathrm{OH}^- \rightarrow [\mathrm{Ag@CeO_2}] + \mathrm{OH}$$

$$[\mathrm{Ag@CeO_2}(\mathrm{h}^+)] + \mathrm{H_2O} \rightarrow [\mathrm{Ag@CeO_2}] + \mathrm{OH}$$

$$\mathrm{OH} + \mathrm{Melanin} \rightarrow \mathrm{Degraded\ Product}$$

Many studies have reported the synthesis and characterization of Ag@CeO_2 NPs but have not delved into the detailed mechanisms underlying their antioxidant and depigmenting effects. Targeting Melanin Production; by reducing oxidative stress within melanocytes, Ag@CeO_2 NPs directly target the melanogenesis pathway. The CeO_2component can directly interact with melanocytes, mitigating ROS-induced activation of tyrosinase, the rate-limiting enzyme in melanin synthesis. These findings align with emerging research on molecular mechanisms driving melanoma progression and pigment regulation. Wang et al. identified ADRA1D as a critical regulator of melanoma angiogenesis and proliferation, suggesting that oxidative stress pathways may intersect with adrenergic signaling to influence tumor behavior. Also, a dual therapeutic strategy was offered by targeting both pigmentation and angiogenesis[42].

On the other side, Ag@CeO_2NPs demonstrate stability under extreme pH and temperature conditions, making them more reliable than natural enzymes or antioxidants. These nanoparticles are cheaper to produce compared to natural antioxidants such as Hydroquinone, Kojic acid, and Ascorbic acid[43], providing a more economical option for therapeutic applications. Furthermore, Ag@CeO_2 nanostructure provides a matrix for the sustained release of Ag and Ce ions. This controlled release prolongs the antioxidant and depigmenting effects, reducing

the need for frequent applications. In the case of the reduced toxicity, encapsulating Ag within the CeO_2 matrix reduces its direct contact with cells, mitigating potential cytotoxicity associated with Ag alone. The CeO_2shell acts as a protective layer, enhancing the biocompatibility of the Ag component[9]. Nanoparticles can be surface-functionalized to selectively target melanocytes, increasing the therapeutic efficacy while minimizing off-target effects. This capability is particularly relevant for treating localized hyperpigmentation[7,44]. Our results showing reduced extracellular melanin content suggest that Ag@CeO_2 NPs could alter the tumor microenvironment, potentially interfering with hMAGEA2-mediated immune evasion. This aligns with Wang et al.[42], who identified ESM1 as a biomarker linked to melanoma proliferation and immune modulation. The antioxidant capacity of Ag@CeO_2 NPs, evidenced by DPPH/ABTS assays, may synergize with ESM1-targeted therapies to suppress immune escape mechanisms. Notably, Zhong et al.[45] classified melanoma subtypes based on PANoptosis genes, emphasizing the interplay between cell death pathways and immune infiltration. The ROS-scavenging ability of Ag@CeO_2 NPs could influence PANoptosis dynamics, as oxidative stress is a key regulator of apoptotic and necroptotic pathways. However, the effects of silver-ceria nanoparticles on melanin synthesis, both in vitro and in vivo, have not yet been reported. This study, however, demonstrated that ceria-silver nanoparticles can effectively reduce melanin levels in the A375 cell line. While Abu-Romman et al.[46] focused on heat-responsive genes in plants, their methodology for characterizing stress-responsive molecular pathways offers a framework for future studies. The hydrothermal synthesis of Ag@CeO_2 NPs in our work parallels their emphasis on thermal stability, highlighting the importance of synthesis parameters in optimizing nanoparticle bioactivity.

Conclusion

Ag@CeO_2 NPs is used as ultraviolet absorbents by photocatalytic activity. In this study, we found this NPs inhibits melanin production in human melanoma cells. Thus, Ag@CeO_2 NPs can potentially be used as a skin-whitening compound for preventing skin darkening in skin care products in the future. Our study provides direct evidence of the melanin-reducing effects of Ag@CeO_2 NPs in A375 melanoma cells, which contributes to filling research gap. Several methods exist to lighten skin pigmentation. For instance, using a sunscreen that contains antioxidants, such as ceria silver nanoparticles, can help protect the skin from free radical damage and inhibit melanin production. Additionally, these nanoparticles significantly inhibit tyrosinase activity and reduce melanin production. They also exhibit extracellular free radical scavenging properties. Nevertheless, a comprehensive understanding of the mechanisms underlying melanogenesis is essential, both from a pharmaceutical and cosmeceutical perspective, to substantiate the observed effects.

Data availability

The datasets used and analyzed during the current study are available from the corresponding author on reasonable request.

Received: 19 February 2025; Accepted: 27 March 2025
Published online: 01 April 2025

References

1. Mohammadi, S. S., Vaezi, Z., Shojaedin-Givi, B. & Naderi-Manesh, H. Chemiluminescent liposomes as a theranostic carrier for detection of tumor cells under oxidative stress. *Anal. Chim. Acta* (2019).
2. Wu, J. Y. et al. Springer,. in *Taurine 7* 169–179 (2009).
3. Dahle, J. T. & Arai, Y. Environmental geochemistry of Cerium: applications and toxicology of cerium oxide nanoparticles. *Int. J. Environ. Res. Public Health*. **12**, 1253–1278 (2015).
4. Xu, C. & Qu, X. Cerium oxide nanoparticle: a remarkably versatile rare Earth nanomaterial for biological applications. *NPG Asia Mater.* **6**, e90–e90 (2014).
5. Sallam, O., Rammah, Y., Nabil, I. M. & El-Seidy, A. M. Enhanced optical and structural traits of irradiated lead Borate glasses via Ce3 + and Dy3 + ions with studying radiation shielding performance. *Sci. Rep.* **14**, 24478 (2024).
6. Hosseini, M. et al. Selective recognition of dysprosium (III) ions by enhanced chemiluminescence CdSe quantum Dots. *Spectrochim. Acta Part A Mol. Biomol. Spectrosc.* **121**, 116–120 (2014).
7. Barbasz, A., Czyżowska, A., Piergies, N. & Oćwieja, M. Design cytotoxicity: the effect of silver nanoparticles stabilized by selected antioxidants on melanoma cells. *J. Appl. Toxicol.* **42**, 570–587 (2022).
8. Adeniyi, O. E., Adebayo, O. A., Akinloye, O. & Adaramoye, O. A. Combined cerium and zinc oxide nanoparticles induced hepato-renal damage in rats through oxidative stress mediated inflammation. *Sci. Rep.* **13**, 8513 (2023).
9. Ramzan, N. et al. Cellular and non-cellular antioxidant properties of vitamin E–loaded metallic-quercetin/polycaprolactone nanoparticles for the treatment of melanogenesis. *AAPS PharmSciTech.* **24**, 141 (2023).
10. Becker, A. L. & Indra, A. K. Oxidative stress in melanoma: beneficial antioxidant and pro-oxidant therapeutic strategies. *Cancers* **15**, 3038 (2023).
11. Zamudio Díaz, D. F. et al. Significance of melanin distribution in the epidermis for the protective effect against UV light. *Sci. Rep.* **14**, 3488 (2024).
12. Guo, L. et al. Recent advances and progress on melanin: from source to application. *Int. J. Mol. Sci.* **24**, 4360 (2023).
13. Kayama, T., Yamazaki, K. & Shinjoh, H. Nanostructured ceria – silver synthesized in a one-pot redox reaction catalyzes carbon oxidation. *J. Am. Chem. Soc.* **132**, 13154–13155 (2010).
14. Göçer, H. & Gülçin, İ. Caffeic acid phenethyl ester (CAPE): correlation of structure and antioxidant properties. *Int. J. Food Sci. Nutr.* **62**, 821–825 (2011).
15. Rajaei, A., Barzegar, M., Mobarez, A. M., Sahari, M. A. & Esfahani, Z. H. Antioxidant, anti-microbial and antimutagenicity activities of pistachio (Pistachia vera) green hull extract. *Food Chem. Toxicol.* **48**, 107–112 (2010).
16. Ali, D., Alarifi, S., Alkahtani, S., AlKahtane, A. A. & Almalik, A. Cerium oxide nanoparticles induce oxidative stress and genotoxicity in human skin melanoma cells. *Cell Biochem. Biophys.* **71**, 1643–1651 (2015).
17. Fu, T., Chai, B., Shi, Y., Dang, Y. & Ye, X. Fargesin inhibits melanin synthesis in murine malignant and immortalized melanocytes by regulating PKA/CREB and P38/MAPK signaling pathways. *J. Dermatol. Sci.* **94**, 213–219 (2019).
18. Foroutan, Z. et al. Plant-based synthesis of cerium oxide nanoparticles as a drug delivery system in improving the anticancer effects of free Temozolomide in glioblastoma (U87) cells. *Ceram. Int.* **48**, 30441–30450 (2022).
19. Tse, G. Computational predictions of CeO2 using HSE03: an Ab initio investigation. *Mod. Phys. Lett. B.* **37**, 2350155 (2023).

20. Khan, M. M. et al. Electrochemically active biofilm assisted synthesis of Ag@ CeO2 nanocomposites for antimicrobial activity, photocatalysis and photoelectrodes. *J. Colloid Interface Sci.* **431**, 255–263 (2014).
21. Amrani, R. et al. Structural and optical properties of highly Ag-doped TiO2 thin films prepared by flash thermal evaporation. *Phys. Scr.* **99**, 065914 (2024).
22. Keshvadi, N., Haghighatzadeh, A. & Mazinani, B. Improvement in visible-light-induced photocatalytic activity of Ag–CeO 2 Schottky-type contact heterostructures. *Appl. Phys. A.* **126**, 1–14 (2020).
23. Sato, R., Takekuma, H. & Teranishi, T. in *Electrochemical Society Meeting Abstracts prime* 3968–3968 (The Electrochemical Society, Inc.). (2024).
24. Saravanakumar, K., Ramjan, M. M., Suresh, P. & Muthuraj, V. Fabrication of highly efficient visible light driven Ag/CeO2 photocatalyst for degradation of organic pollutants. *J. Alloys Compd.* **664**, 149–160 (2016).
25. Jayakumar, G., Irudayaraj, A. A. & Raj, A. D. Particle size effect on the properties of cerium oxide (CeO2) nanoparticles synthesized by hydrothermal method. *Mech. Mater. Sci. Eng. J.* **9** (2017).
26. Ravichandran, V. et al. Green synthesis, characterization, antibacterial, antioxidant and photocatalytic activity of Parkia speciosa leaves extract mediated silver nanoparticles. *Results Phys.* **15**, 102565 (2019).
27. Soren, S., Jena, S. R., Samanta, L. & Parhi, P. Antioxidant potential and toxicity study of the cerium oxide nanoparticles synthesized by microwave-mediated synthesis. *Appl. Biochem. Biotechnol.* **177**, 148–161 (2015).
28. Khan, M., Sohail, Raja, N. I., Asad, M. J. & Mashwani, Z. -u.-R. Antioxidant and hypoglycemic potential of phytogenic cerium oxide nanoparticles. *Sci. Rep.* **13**, 4514 (2023).
29. Athithya, S. et al. Plasmon effect of ag nanoparticles on TiO2/rGO nanostructures for enhanced energy harvesting and environmental remediation. *Nanomaterials* **13**, 65 (2022).
30. Nguyen, T. A. et al. Controlled synthesis of gold nanorods and integrated with titanium dioxide for enhancing visible light-driven antioxidant activity. *Vietnam J. Chem.* **61**, 7–13 (2023).
31. Yong, J. M. et al. ROS-mediated anti-angiogenic activity of cerium oxide nanoparticles in melanoma cells. *ACS Biomaterials Sci. Eng.* **8**, 512–525 (2022).
32. Yi, J. et al. hMAGEA2 as a potential diagnostic and therapeutic target for melanoma progression and metastasis. *Cell. Mol. Biol.* **70**, 97–102 (2024).
33. Phatak, K. A., Khanna, P. K. & Nath, B. B. Silver Oxide Nanoparticles: A Promising Material with Melanin Modulatory Properties Validated in Drosophila. *BioNanoScience*, 1–12 (2024).
34. George, N. & Devi, D. G. Phytonano silver for cosmetic formulation-synthesis, characterization, and assessment of antimicrobial and antityrosinase potential. *Discover Nano*. **19**, 65 (2024).
35. Skoniecka, A., Cichorek, M., Tyminska, A., Pelikant-Malecka, I. & Dziewiatkowski, J. Melanization as unfavorable factor in amelanotic melanoma cell biology. *Protoplasma* **258**, 935–948 (2021).
36. Zhang, D. et al. A multifunctional Low-Temperature photothermal nanomedicine for melanoma treatment via the oxidative stress pathway therapy. *Int. J. Nanomed.*, 11671–11688 (2024).
37. Li, B., Zhang, B., Nie, S., Shao, L. & Hu, L. Optimization of plasmon-induced photocatalysis in electrospun Au/CeO2 hybrid nanofibers for selective oxidation of benzyl alcohol. *J. Catal.* **348**, 256–264 (2017).
38. Zhang, W. et al. Au/Cu2O Schottky contact heterostructures with enhanced photocatalytic activity in dye decomposition and photoelectrochemical water splitting under visible light irradiation. *J. Alloys Compd.* **684**, 445–452 (2016).
39. Ju, X. et al. Poly (acrylic acid)-mediated synthesis of cerium oxide nanoparticles with variable oxidation States and their effect on regulating the intracellular ROS level. *J. Mater. Chem. B.* **9**, 7386–7400 (2021).
40. Tajik, E., Vaezi, Z., Tabarsa, M., Hekmat, A. & Naderi-Manesh, H. Grafting of sinapic acid onto glucosamine nanoparticle as a potential therapeutic drug with enhanced anti-inflammatory activities in osteoarthritis treatment. *Int. J. Biol. Macromol.* **253**, 127454 (2023).
41. Mortazavi, S. M. R., Vaezi, Z., Mahdavian, R., Barzegar, M. & Naderi-Manesh, H. A novel cerasomal Gallic acid as a non-ulcerogenic agent with an improved anti-inflammatory potential. *J. Drug Deliv. Sci. Technol.* **86**, 104610 (2023).
42. Wang, M., Ge, H., Liang, S. & Chen, G. Identification of ESM1 as a potential biomarker involving drug sensitivity and the tumor immune microenvironment that promotes proliferation of melanoma. *Cell. Mol. Biol.* **69**, 160–167 (2023).
43. Pontes, J. F., Fonseca, M., Macedo, A. S., Grenha, A. & Fonte, P. in *Phytopharmaceuticals and Herbal Drugs* 341–373Elsevier, (2023).
44. Fan, P. et al. ZnO nanoparticles stimulate oxidative stress to induce apoptosis of B16F10 melanoma cells: in vitro and in vivo studies. *Biomedical Phys. Eng. Express*. **7**, 065014 (2021).
45. Zhong, L., Qian, W., Gong, W., Zhu, L. & Wang, X. Molecular subtypes based on Panoptosis genes and characteristics of immune infiltration in cutaneous melanoma. *Cell. Mol. Biol.* **69**, 1–8 (2023).
46. Abu-Romman, S. et al. Molecular cloning and characterization of heat-responsive LcOPR1, a gene encoding oxophytodienoic acid reductase in lentil. *Cell. Mol. Biol.* **70**, 1–7 (2024).

Acknowledgements

This research is a part of Masoumeh Ghorbani's PhD dissertation. The authors would like to kindly acknowledge all the support and funding from the research council of Tarbiat Modares University.

Author contributions

M. G.: Conceptualization; data curation; formal analysis; investigation; methodology; validation; visualization; writing—original draft; N. S.: Formal analysis; investigation; visualization methodology; writing—reviewZ. V.: Conceptualization; investigation; validation; writing—reviewD. K.: supervised and conceptualized the study, resources, and funding acquisition.H. N.: Supervision; conceptualization; funding acquisition; project administration.

Declarations

Competing interests

The authors declare no competing interests.

Conflict of interest

The authors declare that they have no conflict of interest.

Additional information

Correspondence and requests for materials should be addressed to Z.V., D.K. or H.N.-M.

Reprints and permissions information is available at www.nature.com/reprints.

Publisher's note Springer Nature remains neutral with regard to jurisdictional claims in published maps and institutional affiliations.

Open Access This article is licensed under a Creative Commons Attribution-NonCommercial-NoDerivatives 4.0 International License, which permits any non-commercial use, sharing, distribution and reproduction in any medium or format, as long as you give appropriate credit to the original author(s) and the source, provide a link to the Creative Commons licence, and indicate if you modified the licensed material. You do not have permission under this licence to share adapted material derived from this article or parts of it. The images or other third party material in this article are included in the article's Creative Commons licence, unless indicated otherwise in a credit line to the material. If material is not included in the article's Creative Commons licence and your intended use is not permitted by statutory regulation or exceeds the permitted use, you will need to obtain permission directly from the copyright holder. To view a copy of this licence, visit http://creativecommons.org/licenses/by-nc-nd/4.0/.

© The Author(s) 2025